Double-Differential Encoding for Dual-Hop Amplify-and-Forward Relaying in IR-UWB Systems

Maziyar Hamdi, Jan Mietzner, and Robert Schober
University of British Columbia, Vancouver, Canada. E-mail: {maziyarh, rschober}@ece.ubc.ca, jan.mietzner@ieee.org

***Abstract*— In this paper, we propose to improve the performance of impulse-radio ultra-wideband (IR-UWB) systems by means of cooperative relaying. With regard to a simple practical realization, we focus on a non-coherent system setup in conjunction with amplify-and-forward (A&F) relaying. In particular, considering a two-hop scenario we propose to employ a double-differential encoding scheme at the source node and single differential decoding at the relay and the destination node, respectively, so as to efficiently limit intersymbol-interference (ISI) effects. A thorough performance analysis of the proposed scheme is provided, along with a closed-form optimization of the transmit power allocation between source and relay. Simulation results illustrate the excellent performance of the proposed scheme, which is compared to alternative coherent and non-coherent schemes based on A&F relaying and decode-and-forward (D&F) relaying.**

I. Introduction

Ultra-wideband (UWB) communication is a wireless spectral underlay technology for transmitting signals with a bandwidth larger than 500 MHz or a fractional bandwidth of more than 20% [1]. In impulse-radio UWB (IR-UWB) systems, the transmitted signal consists of a train of pulses of very short duration (on the order of nanoseconds) [2]. Due to its simple practical realization and its robustness to multipath fading and intersymbol-interference (ISI) effects, IR-UWB has attracted considerable attention.

In order to limit interference to incumbent wireless services, the US Federal Communications Commission (FCC) has issued tight restrictions on the transmitted power spectral density (PSD) of UWB systems [3]. Because of these limitations, it is indispensable to capture most of the signal energy provided by the large number of resolvable multipath components. A favorable property of IR-UWB systems is that they allow for an efficient energy combining at the receiver [4] – either by means of coherent Rake combining [5] or non-coherent energy detection schemes [6]. While Rake combining offers optimum performance in terms of bit error rate (BER), it requires accurate channel estimation at the receiver and precise synchronization, which might be challenging in practice. In particular, a large number of "Rake fingers" is typically required in order to capture most of the signal energy [7]. As opposed to this, non-coherent energy detection schemes relieve the receiver from any channel estimation task and are thus easier to realize. They capture the energy of the multipath components by means of an autocorrelation of the received signal, followed by an integrate-and-dump operation. Among these techniques, differential (DF) and transmitted-reference (TR) schemes are the most popular options [6]. A notable advantage of the DF scheme is that it offers a higher data rate compared to a TR scheme. In the literature, several methods have been proposed to improve the performance of DF schemes, such as reference filtering [8], weighted correlation [9], and multiple symbol detection [10].

In this paper, we investigate cooperative relaying as an alternative option, which was shown to be an excellent means to overcome the limited coverage of (coherent or non-coherent) UWB systems [11], [12]. Instead of transmitting signals directly from a source node, S, to a destination node, D, the signal is (in the simplest case) received by an intermediate relay, R, which forwards the received signal to the destination. By this means, substantial path-loss gains can be provided due to shorter link lengths. Two popular algorithms for cooperative relaying are amplify-and-forward (A&F) and decode-and-forward (D&F). A&F relays simply amplify and re-transmit the received signal, whereas D&F relays first decode and then re-encode the received signal, before re-transmission is performed [13]. Correspondingly, D&F relaying is more complex, especially if a forward-error-correction (FEC) code is employed.

Here, we focus on a non-coherent two-hop IR-UWB system that is based on A&F relaying. In particular, we propose to employ a double-differential encoding scheme at the source node in conjunction with single differential decoding at the A&F relay and the destination node, respectively, so as to efficiently limit ISI effects. To the best of our knowledge, such a use of double-differential encoding is novel and quite different from narrowband systems, where double-differential encoding is employed to mitigate carrier frequency offsets [14]. A major advantage of our scheme is that the size of the guard interval necessary to avoid ISI does not have to be increased compared to direct transmission. In comparison, in order to achieve a similar level of ISI, a simple A&F-relaying scheme with single differential encoding at the source node and differential decoding only at the destination node would require significantly larger guard intervals between the transmitted pulses, due to an increased length of the effective overall channel impulse response (CIR). This would significantly lower the effective transmission rate compared to the case of direct transmission.

The remainder of the paper is organized as follows. In Section II, we describe the system setup under consideration. In Section III, we provide a thorough performance analysis of our proposed scheme, along with a closed-form optimization of the transmit power allocation between source node and relay. Simulation results illustrating the excellent performance of our scheme, are presented in Section IV. Finally, Section V concludes the paper and presents directions for future work.

II. System Model

We consider a single-user scenario throughout this paper. Fig. 1 shows the block diagrams of the source node S, the relay R, and the destination node D.

A. Source Node

At the source node, the information bits $d[k] \in \{\pm 1\}$ are first double-differentially encoded according to

$$q[k] = d[k]q[k-1], \qquad b[k] = q[k]b[k-1], \tag{1}$$

where $q[k] \in \{\pm 1\}$ and $b[k] \in \{\pm 1\}$ denote the kth intermediate symbol after the first and second differential encoder, respectively. The symbols $b[k]$ are then modulated onto a train of short pulses $w_{tx}(t)$ with duration T_p, according to [1]

$$s_1(t) = \sqrt{\alpha_1 E_g} \sum_{k=-\infty}^{\infty} \sum_{j=0}^{N_f-1} b[k]\, w_{tx}(t - jT_f - kT_s). \quad (2)$$

Here, $s_1(t)$ denotes the transmitted signal, α_1 the transmit power allocation factor for the source node, E_g the energy per pulse ($\int_{-\infty}^{+\infty} w_{tx}^2(t)\, dt := 1$), N_f the number of frames used for conveying a single information bit, T_f the frame duration, and $T_s = N_f T_f$ the symbol duration. The length of the guard interval between pulses, $T_g = T_f - T_p$, is typically chosen longer than the length of the underlying UWB CIR (source-relay link in this case), so as to circumvent ISI effects.

B. Channel Model

In the following, we denote the source-relay link as link 1 and the relay-destination link as link 2. For all links under consideration, we employ the IEEE 802.15.3a channel models [15] for UWB personal area networks. Consequently, the passband version of the CIR of the rth link consists of L_C clusters of L_R rays and is modeled as

$$h_r(t) = \sum_{\nu=0}^{L_C} \sum_{\mu=0}^{L_R} \lambda_{\mu,\nu}^{(r)}\, \delta(t - T_\nu^{(r)} - \tau_{\mu,\nu}^{(r)}), \quad (3)$$

where $\lambda_{\mu,\nu}^{(r)}$ models the random multipath gain coefficient of the μth ray of the νth cluster, $T_\nu^{(r)}$ the delay of the νth cluster, $\tau_{\mu,\nu}^{(r)}$ the delay of the μth ray of the νth cluster, and $\delta(\cdot)$ denotes a Dirac impulse. The multipath gain coefficients are normalized such that $\sum_{\nu=0}^{L_C} \sum_{\mu=0}^{L_R} (\lambda_{\mu,\nu}^{(r)})^2 = 1$. In [15], four different parameter sets are specified for the various parameters in (3). The resulting channel models, CM1-CM4, represent different usage scenarios and entail different amounts of ISI.

The channel gain is affected by log-normal fading and path loss. In the following, the source-destination link will serve as the reference link for the path loss. Assuming omni-directional antennas at all nodes, the relative channel gain associated with the rth link is thus modeled by a factor [12]

$$A_r = X_r \left(\frac{d_{S-D}}{d_r} \right)^p, \quad (4)$$

where X_r models log-normal shadowing, d_{S-D} and d_r denote the length of the source-destination link and the rth link, respectively, and p denotes the path-loss exponent, which is typically between $1.7 \leq p \leq 3.5$ [15]. Throughout this paper, we assume that the lognormal shadowing terms X_r and $X_{r'}$ associated with two different links $r \neq r'$ are uncorrelated.

C. A&F Relay

At the receiver front-end of the relay, the received signal is first passed through a bandpass filter $h_{BP}(t)$ with one-sided bandwidth W, so as to eliminate out-of-band noise. The

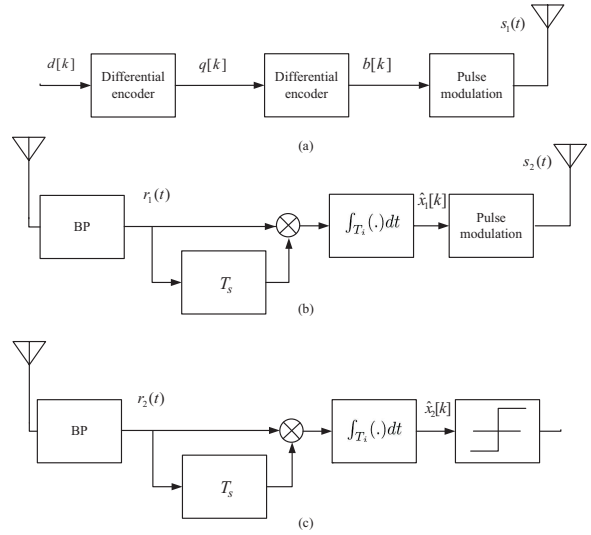

Fig. 1. Block diagram of (a) the source node S, (b) the A&F relay R, and (c) the destination node D.

filtered received signal at the relay is given by

$$\begin{aligned} r_1(t) &= \sqrt{A_1}\,(h_1(t) * h_{BP}(t)) * s_1(t) + n_1(t) \\ &= \sqrt{A_1 \alpha_1 E_g} \sum_{k=-\infty}^{\infty} \sum_{j=0}^{N_f-1} b[k]\, w_{rx,1}(t - jT_f - kT_s) \\ &\quad + n_1(t), \end{aligned} \quad (5)$$

where A_1 is the relative channel gain of the source-relay link ($r=1$), $h_1(t)$ the corresponding CIR, $w_{rx,1}(t) = w_{tx}(t) * h_1(t) * h_{BP}(t)$ the received pulse, $n_1(t)$ the filtered additive white Gaussian noise (AWGN) with zero mean and single-sided noise PSD $\frac{N_0}{2}$, and '$*$' denotes linear convolution. For the numerical results presented in Section IV, the bandwidth W of $h_{BP}(t)$ was optimized numerically for maximization of the received signal-to-noise ratio (SNR).

After the bandpass filter, (single) differential decoding of the filtered signal $r_1(t)$ is performed. To this end, $r_1(t)$ is first delayed by a symbol duration T_s and is multiplied by itself, as shown in Fig. 1 (b). The resulting signal $r_1(t) r_1(t - T_s)$ is passed through an integrator with integration duration T_i.[1] The integrator yields the discrete-time sample

$$\hat{x}_1[k] = \sum_{j=0}^{N_f-1} \int_{kT_s + jT_f}^{kT_s + +jT_f + T_i} r_1(t) r_1(t - T_s) dt, \quad (6)$$

which can be interpreted as a (soft) estimate of the intermediate symbol $q[k]$. Similar to (2), the estimated symbols $\hat{x}_1[k]$ are finally modulated onto a signal

$$s_2(t) = \sqrt{\alpha_2 E_g} \sum_{k=-\infty}^{\infty} \sum_{j=0}^{N_f-1} \hat{x}_1[k]\, w_{tx}(t - jT_f - kT_s), \quad (7)$$

which is then re-transmitted to the destination node. Here, α_2 denotes the power allocation factor for the relay node.

[1] Similar to the filter bandwidth W, the integration duration T_i has to be optimized such that (on average) most of the signal energy is captured, while the collected noise energy is kept to a minimum.

In the case of D&F relaying, a hard decision on the symbols $\hat{x}_1[k]$ would be performed prior to re-transmission (followed by an FEC decoding step, if a coded system is considered).

D. Destination Node

The receiver structure of the destination node is identical to that of the relay. In particular, we assume an identical bandpass filter $h_{BP}(t)$ for simplicity. Similar to (5), the filtered received signal is given by

$$\begin{aligned} r_2(t) &= \sqrt{A_2}\,(h_2(t) * h_{BP}(t)) * s_2(t) + n_2(t) \\ &= \sqrt{A_2\alpha_2 E_g} \sum_{k=-\infty}^{\infty} \sum_{j=0}^{N_f-1} \hat{x}_1[k]\; w_{rx,2}(t - jT_f - kT_s) \\ &\quad + n_2(t), \end{aligned} \tag{8}$$

where $w_{rx,2}(t) := w_{tx}(t) * h_2(t) * h_{BP}(t)$ and $h_2(t)$ denotes the CIR of the relay-destination link ($r=2$). In order to recover the transmitted information bits $d[k]$, the destination node performs another differential decoding step. This yields estimated symbols

$$\hat{x}_2[k] = \sum_{j=0}^{N_f-1} \int_{kT_s+jT_f}^{kT_s+jT_f+T_i} r_2(t) r_2(t-T_s)dt \tag{9}$$

(cf. Fig. 1 (c)), which are passed through a slicer, in order to arrive at the final (hard) estimates $\hat{d}[k]$ of the transmitted information bits $d[k]$.

III. Performance Analysis

In the following, we provide a thorough performance analysis of the proposed system setup. In particular, we show that the input-output behavior of the system can be described as

$$\hat{x}_2[k] = \tilde{\beta}_2\, d[k] + w_2[k], \tag{10}$$

where $\tilde{\beta}_2$ and $w_2[k]$ represent a gain factor and an effective noise sample, respectively. We note that $w_2[k]$ is in general non-Gaussian, and thus, an accurate analysis of the resulting BER seems difficult. Therefore, we focus on the effective SNR at the destination node in this section. In particular, we derive a closed-form expression for the SNR at the destination node and use this expression for optimization of the power allocation factors α_1 and α_2 for the source node and the A&F relay, respectively.

A. Effective SNR at the Destination Node

We start by substituting $r_1(t)$ from (5) into (6) and get

$$\hat{x}_1[k] = \beta_1 \overbrace{b[k]b[k-1]}^{q[k]} + z_1[k] + z_2[k] + z_3[k], \tag{11}$$

where $\beta_1 := N_f A_1 \alpha_1 \varepsilon_1$, $\varepsilon_1 := E_g \int_0^{T_i} w_{rx,1}^2(t)dt$, and $z_1[k]$, $z_2[k]$, and $z_3[k]$ are zero-mean noise terms defined as follows:

$$\begin{aligned} z_1[k] &= b[k]\sqrt{A_1\alpha_1 E_g} \\ &\quad \times \sum_{j=0}^{N_f-1} \int_{kT_s}^{kT_s+T_i} n_1(t-T_s) w_{rx,1}(t - jT_f - kT_s)dt, \end{aligned} \tag{12}$$

$$\begin{aligned} z_2[k] &= b[k-1]\sqrt{A_1\alpha_1 E_g} \\ &\quad \times \sum_{j=0}^{N_f-1} \int_{kT_s}^{kT_s+T_i} n_1(t) w_{rx,1}(t - jT_f - (k-1)T_s)dt, \end{aligned} \tag{13}$$

$$z_3[k] = \int_{kT_s}^{kT_s+T_i} n_1(t) n_1(t-T_s)dt. \tag{14}$$

As described earlier, $n_1(t)$ and $n_2(t)$ are obtained by filtering corresponding AWGN processes with single-sided noise PSD $\frac{N_0}{2}$ with a bandpass filter with one-sided bandwidth W. The corresponding autocorrelation function (ACF) $\phi_i(\tau)$ ($i=1,2$) is thus given by [16]

$$\phi_i(\tau) = E\{n_i(t)n_i(t-\tau)\} = \frac{N_0}{2} \cdot \frac{\sin(\pi W \tau)}{\pi W \tau} \cos(2\pi f_0 \tau) \tag{15}$$

($i=1,2$), where f_0 denotes the center frequency of the bandpass filter, and $E\{\cdot\}$ denotes statistical expectation. Assuming that the bandwidth W is chosen sufficiently large, such that the frequency response of the received pulse $w_{rx,1}(t)$ falls completely inside the PSD $\Phi_1(f)$ of $n_1(t)$, and the PSD $\Phi_1(f)$ is sufficiently flat in the area of interest, the ACF $\phi_1(\tau)$ can be replaced by $\frac{N_0}{2}\delta(\tau)$. Thus, the variances of the noise terms $z_1[k]$, $z_2[k]$, and $z_3[k]$ can be approximated as

$$\begin{aligned} \sigma_{z_1}^2 &= E\{z_1^2[k]\} \\ &= N_f A_1 \alpha_1 E_g \int_0^{T_i}\int_0^{T_i} w_{rx,1}(t) w_{rx,1}(\tau) \phi_1(t-\tau) dt d\tau \\ &\approx N_f A_1 \alpha_1 E_g \frac{N_0}{2} \int_0^{T_i} w_{rx,1}^2(t)dt = \beta_1 \frac{N_0}{2}, \end{aligned} \tag{16}$$

$$\sigma_{z_2}^2 = E\{z_2^2[k]\} = \sigma_{z_1}^2, \tag{17}$$

$$\begin{aligned} \sigma_{z_3}^2 &= E\{z_3^2[k]\} = \int_0^{T_i}\int_0^{T_i} \phi_1^2(t-\tau) dt d\tau \\ &= \int_0^{T_i}\int_{T_i-t}^{T_i} \phi_1^2(u) dt du, \\ &= \int_0^{T_i} \frac{N_0^2}{4} \cdot 2 \cdot W dt = \frac{W T_i N_0^2}{2}. \end{aligned} \tag{18}$$

In (18), we have exploited the fact that the integrand $\phi_1^2(u)$ is Dirac-like, i.e., the integral vanishes outside $[-t, T_i - t]$, and have employed Parseval's theorem to calculate the integral.

In the following, let $w_1[k] := z_1[k] + z_2[k] + z_3[k]$ denote the effective noise sample at the integrator output of the relay. Thus, we have

$$\hat{x}_1[k] = \beta_1 q[k] + w_1[k], \tag{19}$$

where $w_1[k]$ has zero mean and variance $\sigma_1^2 := \beta_1 N_0 + \frac{W T_i N_0^2}{2}$. Note that $w_1[k]$ is not Gaussian distributed since $z_3[k]$ is not Gaussian.

Along the same lines, we can analyze the integrator output of the destination node. Substituting (8) into (9) yields

$$\hat{x}_2[k] = \beta_2 \hat{x}_1[k]\hat{x}_1[k-1] + z_1'[k] + z_2'[k] + z_3'[k], \tag{20}$$

where $\beta_2 := N_f A_2 \alpha_2 \varepsilon_2$, $\varepsilon_2 := E_g \int_0^{T_i} w_{rx,2}^2(t)dt$, and $z_1'[k]$, $z_2'[k]$, and $z_3'[k]$ are similarly defined as in (12), with $b[k]$ being replaced by $\hat{x}_1[k]$, A_1 by A_2, α_1 by α_2, $n_1(t)$ by $n_2(t)$,

and $w_{rx,1}(t)$ by $w_{rx,2}(t)$. Plugging in $\hat{x}_1[k]$ from (19), we get

$$\hat{x}_2[k] = \beta_2\beta_1^2 \overbrace{q[k]q[k-1]}^{d[k]} + z_4'[k] + z_5'[k] + z_6'[k] + w_2'[k], \quad (21)$$

where $w_2'[k] := z_1'[k] + z_2'[k] + z_3'[k]$, and $z_4'[k]$, $z_5'[k]$, and $z_6'[k]$ are defined as

$$\begin{aligned} z_4'[k] &= \beta_2\beta_1 q[k]w_1[k-1], \\ z_5'[k] &= \beta_2\beta_1 q[k-1]w_1[k], \\ z_6'[k] &= \beta_2 w_1[k]w_1[k-1]. \end{aligned} \quad (22)$$

The variance of $z_1'[k]$, $z_2'[k]$, and $z_3'[k]$ can be calculated similarly to (16)–(18). One obtains

$$\begin{aligned} \sigma_{z_1'}^2 &\approx E\{\hat{x}_1^2[k]\}\beta_2\frac{N_0}{2} = (\beta_1^2+\sigma_1^2)\beta_2\frac{N_0}{2}, \\ &\sigma_{z_2'}^2 = \sigma_{z_1'}^2, \quad \sigma_{z_3'}^2 = \sigma_{z_3}^2. \end{aligned} \quad (23)$$

The variance of $z_4'[k]$, $z_5'[k]$, and $z_6'[k]$ can be calculated from (22):

$$\sigma_{z_4'}^2 = \sigma_{z_5'}^2 = (\beta_2\beta_1)^2\sigma_1^2 \quad \text{and} \quad \sigma_{z_6'}^2 \approx \beta_2^2\sigma_1^4. \quad (24)$$

For computing the variance of $z_6'[k]$, we have assumed that $w_1[k]$ and $w_1[k-1]$ are statistically independent.

Based on (21)–(24), we are now ready to obtain the input-output behavior of our system according to (10), where $\tilde{\beta}_2 := \beta_2\beta_1^2$ and $w_2[k] := z_4'[k] + z_5'[k] + z_6'[k] + w_2'[k]$. In order to calculate the variance of $w_2[k]$ we should note that $z_4'[k]$ and $z_5'[k]$ are not mutually independent, i.e., their correlation cannot be ignored. In particular, one finds that

$$\begin{aligned} E\{z_4'[k]z_5'[k]\} &= (\beta_2\beta_1)^2 E\{q[k]q[k-1]w_1[k]w_1[k-1]\} \\ &= (\beta_2\beta_1)^2 E\{q[k]q[k-1]z_1[k]z_2[k-1]\}. \end{aligned} \quad (25)$$

A careful look at (12) and (13) reveals that $b[k-2]z_2[k-1] = b[k]z_1[k]$. Thus, we have $E\{q[k]q[k-1]z_1[k]z_2[k-1]\} = E\{b[k]b[k-2]z_1[k]z_2[k-1]\} = E\{z_1^2[k]\} = \beta_1\frac{N_0}{2}$ and get

$$E\{z_4'[k]z_5'[k]\} = \beta_2^2\beta_1^3\frac{N_0}{2}. \quad (26)$$

Based on (21)–(26), the effective SNR at the destination node can be calculated as

$$\begin{aligned} \text{SNR} &= \frac{(\beta_2\beta_1^2)^2}{\sigma_{z_4'}^2 + \sigma_{z_5'}^2 + \sigma_{z_6'}^2 + 2E\{z_4'[k]z_5'[k]\} + \sigma_{w_2'}^2} \quad (27) \\ &= \frac{(\beta_2\beta_1^2)^2}{\beta_2^2(2\beta_1^2\sigma_1^2 + \beta_1^3 N_0 + \sigma_1^4) + \beta_2 N_0(\beta_1^2+\sigma_1^2) + \frac{WT_iN_0^2}{2}}. \end{aligned}$$

B. Optimized Transmit Power Allocation

Based on (27), we can now optimize the transmit power allocation factors α_1 and α_2 for the source node and the A&F relay, respectively. We aim to maximize the effective SNR at the destination node, under the constraint of keeping the total transmit power fixed.

It can be shown that the total transmit power constraint can be expressed as

$$\alpha_1 + \alpha_2(\beta_1^2 + \sigma_1^2) \stackrel{!}{=} 1. \quad (28)$$

Concerning (27), we can make a high-SNR approximation, according to

$$\text{SNR} \approx \frac{\beta_2\beta_1^2}{\beta_2(2\sigma_1^2 + \beta_1 N_0) + N_0}, \quad (29)$$

where we have used that, for high SNR, $2\beta_1^2\sigma_1^2 + \beta_1^3 N_0 \gg \sigma_1^4$, $\beta_1^2 \gg \sigma_1^2$, and $\frac{WT_iN_0^2}{2}$ becomes negligible.

Assuming again high SNR, we can now formulate the Lagrange problem

$$\Lambda(\alpha_1, \alpha_2, \gamma) = \frac{\beta_2\beta_1^2}{(3\beta_1\beta_2 + 1)N_0} - \gamma(\alpha_1 + \alpha_2\beta_1^2 - 1), \quad (30)$$

where γ denotes the Lagrange multiplier and we have used the high-SNR approximations $\beta_1^2 \gg \sigma_1^2$ and $\sigma_1^2 \approx \beta_1 N_0$. Based on (30), the optimal transmit power allocation results as

$$\alpha_{1,\text{opt}} = \frac{1}{1 + \sqrt{\frac{A_1}{3A_2}}}, \qquad \alpha_{2,\text{opt}} = \frac{1 - \alpha_{1,\text{opt}}}{\beta_1^2 + \sigma_1^2}, \quad (31)$$

which only depends on the link gains A_1 and A_2.

IV. Numerical Performance Results

In the following, we present numerical performance results, which illustrate the excellent performance of our proposed scheme and corroborate our analysis in Section III. Throughout this section, the information bits $d[k] \in \{\pm 1\}$ are transmitted in blocks of 1000 bits. For simplicity, channel coding is not applied. The CIR is assumed to remain static for the duration of an entire block ($70\,\mu s$). As an example, we focus on channel model CM1 in the sequel and assume a path-loss exponent of $p = 3$. One frame is used for transmitting a single information bit ($N_f = 1$), and the frame length is chosen such that the guard interval between subsequent pulses is larger than the root-mean-square (rms) delay spread of the channel ($T_f = 70\,ns$), so as to circumvent ISI effects. For the transmitted pulse $w_{tx}(t)$, we employ the widely-used second derivative of a Gaussian pulse, i.e.,

$$w_{tx}(t) = [1 - 4\pi(t - v_p)/v_m^2]\exp[-2\pi((t - v_p)/v_m)^2],$$

where $v_p = 0.35\,ns$ and $v_m = 0.2877\,ns$ ($T_p = 0.7\,ns$). The bandwidth W of the bandpass filter is optimized such that the maximum received SNR is obtained ($W = 5$ GHz). Moreover, the integration time T_i has been optimized such that on average the maximum effective SNR at the integrator output is obtained ($T_i = 5.25\,ns$).

Fig. 2 shows the effective SNR at the destination node for the double-differential A&F-relaying scheme for $E_g/N_0 = 9$ dB, considering three different positions of the relay ($\rho := d_1/d_{S-D} = \{0.2, 0.4, 0.6\}$, where d_1 and d_{S-D} denote the length of the source-relay and the source-destination link, respectively). Analytical results based on (27) are represented by lines, and corresponding simulation results are represented by markers. Moreover, the cross signs indicate the optimum value for α_1, which was found based on (31). As can be seen, the analytical and the simulation results fit well, and considering the fact that our (approximate) formula (31) was derived for high SNR values whereas the SNR for Fig. 2 is moderate, the optimal power allocation factor $\alpha_{1,\text{opt}}$ obtained with (31) offers a remarkable accuracy.

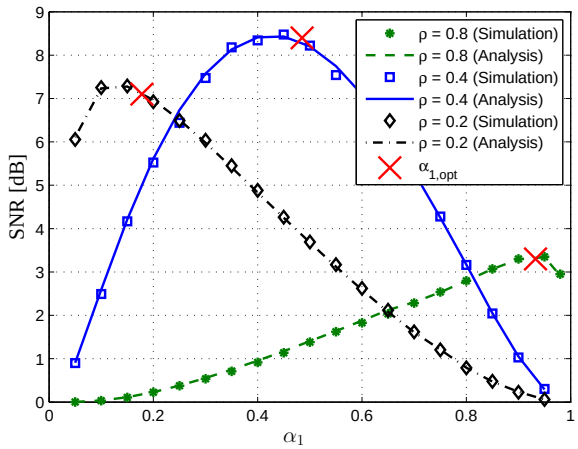

Fig. 2. Effective SNR at the destination node versus transmit power allocation factor α_1 for the source node (three different values for the source-relay link length are considered).

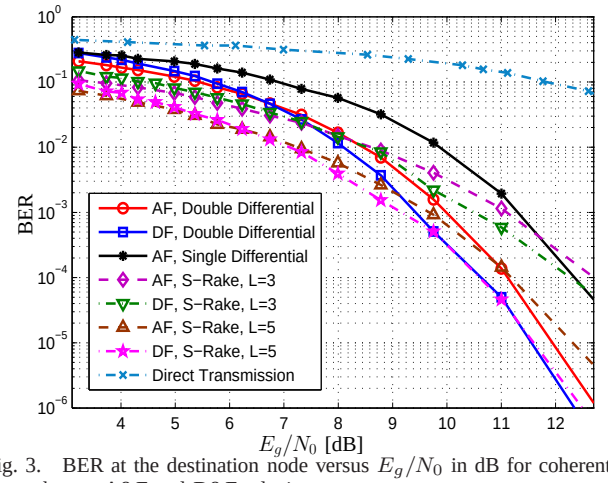

Fig. 3. BER at the destination node versus E_g/N_0 in dB for coherent and non-coherent A&F and D&F relaying.

Fig. 3 illustrates the performance of the proposed non-coherent A&F relaying scheme with double-differential encoding at the source node, obtained by means of Monte-Carlo simulations over a large number of independent CIR realizations for $\rho = 0.2$. The proposed scheme is compared with (i) direct transmission from the source to the destination node, (ii) non-coherent A&F relaying with single differential encoding at the source node, (iii) coherent A&F and D&F relaying with S-Rake (Selective Rake) reception at the relay and at the destination node ($L = 3, 5$ Rake-fingers), and (iv) non-coherent D&F relaying scheme with double-differential encoding at the source node. α_1 and α_2 were optimized based on (31) for the proposed A&F relaying scheme with double-differential encoding and based on simulations for the other relaying schemes. As can be seen, all considered relaying schemes offer remarkable improvements over the case of direct transmission. Moreover, at sufficiently high SNR our proposed scheme outperforms the coherent A&F and D&F relaying schemes, unless a relatively large number of Rake fingers is employed (e.g., $L \geq 5$). The double-differential D&F-relaying scheme offers a small performance advantage of about 0.5 dB compared to the A&F version, at the expense of an increased relay complexity. A&F relaying with straightforward single-differential encoding at the source, amplification at the relay, and differential decoding at the destination suffers from a significant loss in performance compared to the proposed scheme. We have doubled the integration time T_i at the destination for A&F relaying with single-differential encoding, since the effective CIR seen at the destination is the convolution of the CIRs of the source-relay and the relay-destination channels. Therefore, the length of the effective CIR is roughly doubled compared to the proposed scheme. We note that the performance of A&F relaying with single-differential encoding could be improved by increasing the frame duration T_f at the expense of a loss in data rate.

V. Conclusion

We proposed a double-differential encoding scheme for two-hop A&F relaying in IR-UWB systems. After a thorough performance analysis of the proposed scheme, a closed-form solution for the optimum transmit power allocation between source node and relay was derived. Simulation results showed that the proposed A&F-relaying scheme offers an excellent performance and can even compete with coherent A&F and D&F-relaying schemes that are based on S-Rake combining. For future work, it will be interesting to extend the presented framework to the case of multi-hop relaying IR-UWB systems using multi-differential encoding at the source node and single differential decoding at each relay and at the destination node.

References

[1] L. Yang and G. Giannakis, "Ultra-wideband communications: an idea whose time has come," *Signal Processing Magazine, IEEE*, vol. 21, no. 6, pp. 26–54, Nov. 2004.

[2] M. Win and R. Scholtz, "Impulse radio: how it works," *IEEE Commun. Letters*, vol. 2, pp. 36–38, Jan. 1998.

[3] Federal Communications Commission (FCC), "Revision of part 15 of the commission's rules regarding ultra-wideband transmission systems," First Report and Order, ET Docket 98–153, FCC 02–48; Adopted: February 2002; Released: March 2003.

[4] M. Win and R. Scholtz, "On the energy capture of ultrawide bandwidth signals in dense multipath environments," *IEEE Commun. Letters*, vol. 2, pp. 245–247, Sep 1998.

[5] A. Rajeswaran, V. Somayazulu, and J. Foerster, "Rake performance for a pulse based UWB system in a realistic UWB indoor channel," in *Proc. IEEE Intern. Conf. Commun. (ICC)*, May 2003, pp. 2879–2883.

[6] N. He and C. Tepedelenlioglu, "Performance analysis of non-coherent UWB receivers at different synchronization levels," *IEEE Trans. Wireless Commun.*, vol. 5, pp. 1266–1273, June 2006.

[7] D. Cassioli, M. Win, F. Vatalaro, and A. Molisch, "Performance of low-complexity rake reception in a realistic UWB channel," in *Proc. IEEE Intern. Conf. Commun. (ICC)*, 2002, pp. 763–767.

[8] S. Zhao, H. Liu, and Z. Tian, "A decision-feedback autocorrelation receiver for pulsed ultra-wideband systems," in *Proc. IEEE Radio and Wireless Conference*, Sept. 2004, pp. 251–254.

[9] J. Romme and G. Durisi, "Transmit reference impulse radio systems using weighted correlation," in *Proc. Intern. Workshop on Ultra Wideband Systems*, May 2004, pp. 141–145.

[10] N. Guo and R. Qiu, "Improved autocorrelation demodulation receivers based on multiple-symbol detection for UWB communications," *IEEE Trans. Wireless Commun.*, vol. 5, pp. 2026–2031, Aug. 2006.

[11] W. Siriwongpairat, W. Su, Z. Han, and K. Liu, "Employing cooperative diversity for performance enhancement in UWB communication systems," in *Proc. IEEE Wireless Commun. and Networking Conf., (WCNC)*, vol. 4, April 2006, pp. 1854–1859.

[12] J. Kan, J. Mietzner, C. Snow, and R. Schober, "Enhancement of the ECMA-368 UWB system by means of compatible relaying techniques," in *Proc. Intern. Conf. Ultra-Wideband (ICUWB)*, Sept. 2008, pp. 63–67.

[13] J. N. Laneman, "Cooperative diversity in wireless networks: Algorithms and architectures," Ph.D. dissertation, Massachusetts Institute of Technology, September 2002.

[14] M. Simon and D. Divsalar, "On the implementation and performance of single and double differential detection schemes," *IEEE Trans. Commun.*, vol. 40, pp. 278–291, Feb 1992.

[15] A. Molisch, J. Foerster, and M. Pendergrass, "Channel models for ultrawideband personal area networks," *IEEE Wireless Commun.*, vol. 10, pp. 14–21, Dec. 2003.

[16] J. Proakis, *Digital Communications*. New York: McGraw Hill, 2001.